Supporting Information

Luminescent Cyclometalated Platinum(II) Complexes with Acyclic Diaminocarbene Ligands: Structural, Photophysical and Biological Properties

Mónica Martínez-Junquera,[a] Elena Lalinde,[a] M. Teresa Moreno,[a] Elvira Alfaro-Arnedo,[b] Icíar P. López,[b] Ignacio M. Larráyoz[c] and José G. Pichel*,[b,d]*

[a] Departamento de Química-Centro de Síntesis Química de La Rioja, (CISQ), Universidad de La Rioja, 26006, Logroño, Spain. E-mail: teresa.moreno@unirioja.es

[b] Lung Cancer and Respiratory Diseases Unit (CIBIR), Fundación Rioja Salud, 26006 Logroño, Spain. E-mail: jgpichel@riojasalud.es

[c] Biomarkers and Molecular Signaling Unit (CIBIR), Fundación Rioja Salud, 26006 Logroño, Spain.

[d] Biomedical Research Networking Center in Respiratory Diseases (CIBERES), ISCIII, Spain.

Contents: **Page**

1.- Characterization of complexes

1.1- Mass spectra

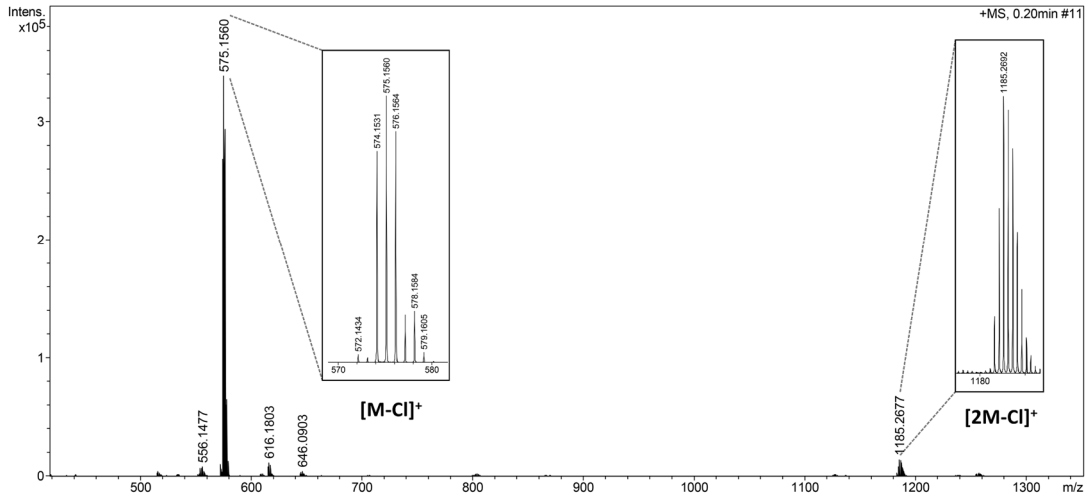

(a)

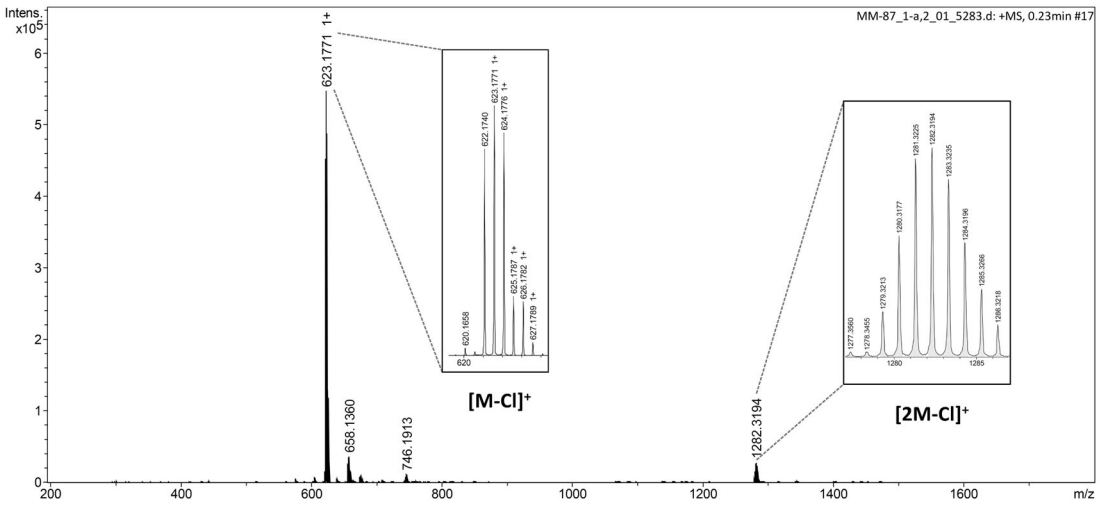

(b)

Figure S1.- ESI$^+$-MS spectra of **3a** (a) and **3b** (b).

1.2- NMR Spectra

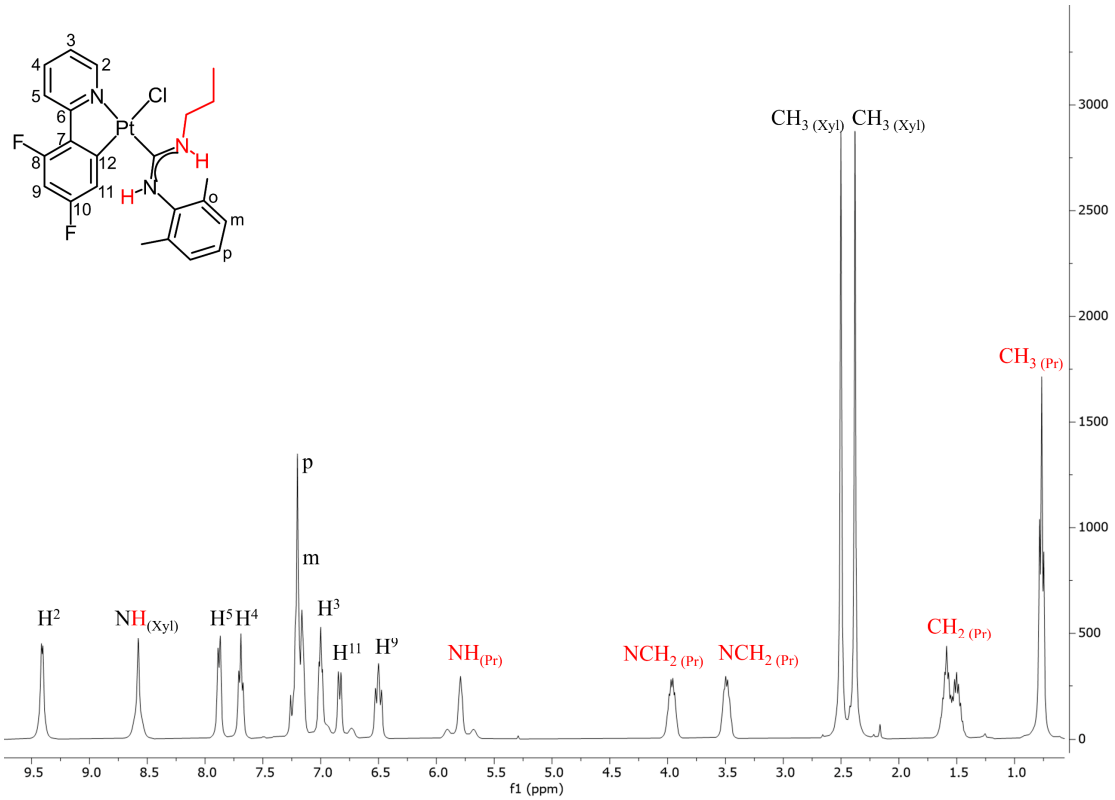

(a)

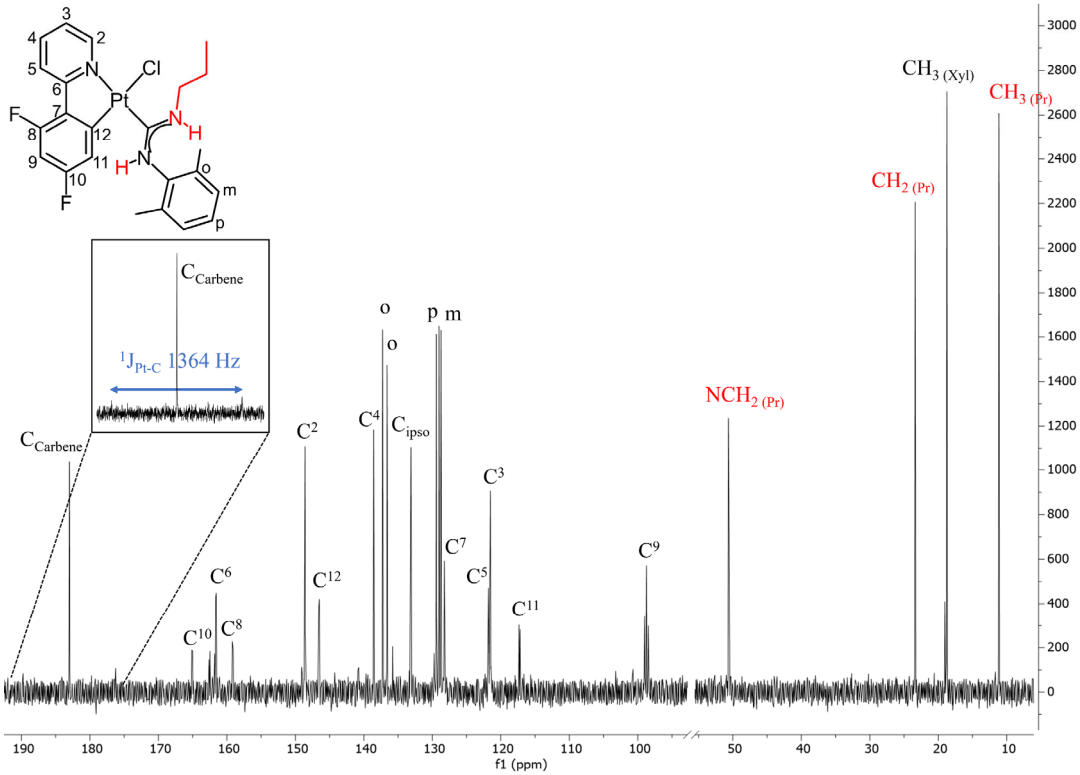

(b)

Figure S2. NMR spectra of **3a** in $CDCl_3$ at 298 K, (a) ^1H, (b) $^{13}C\{^1H\}$ at 0.1 M.

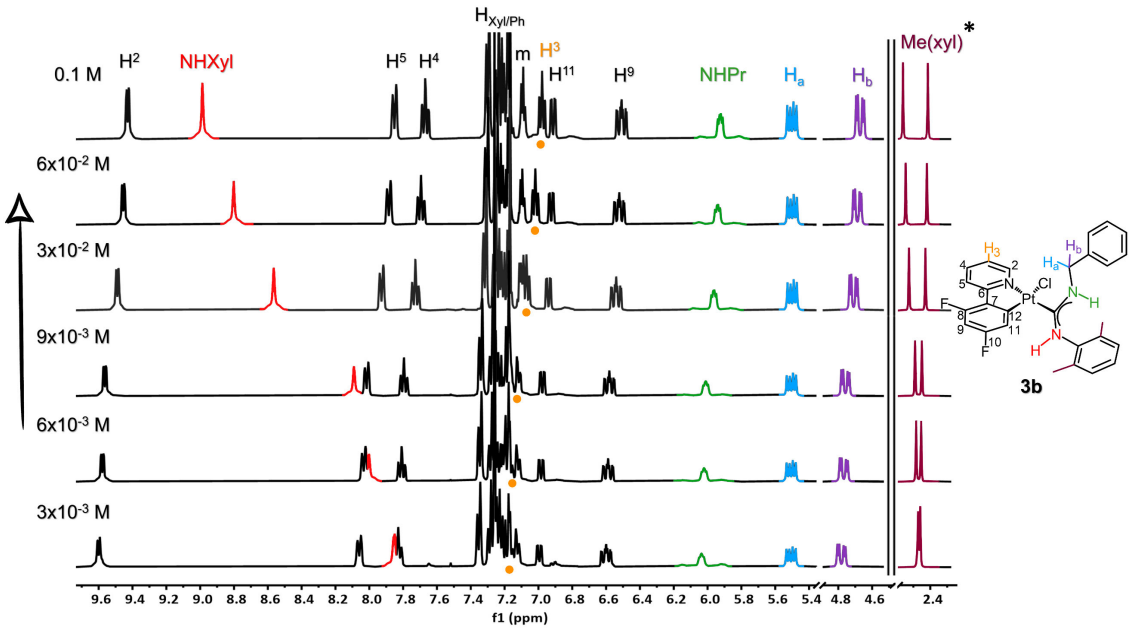

(a)

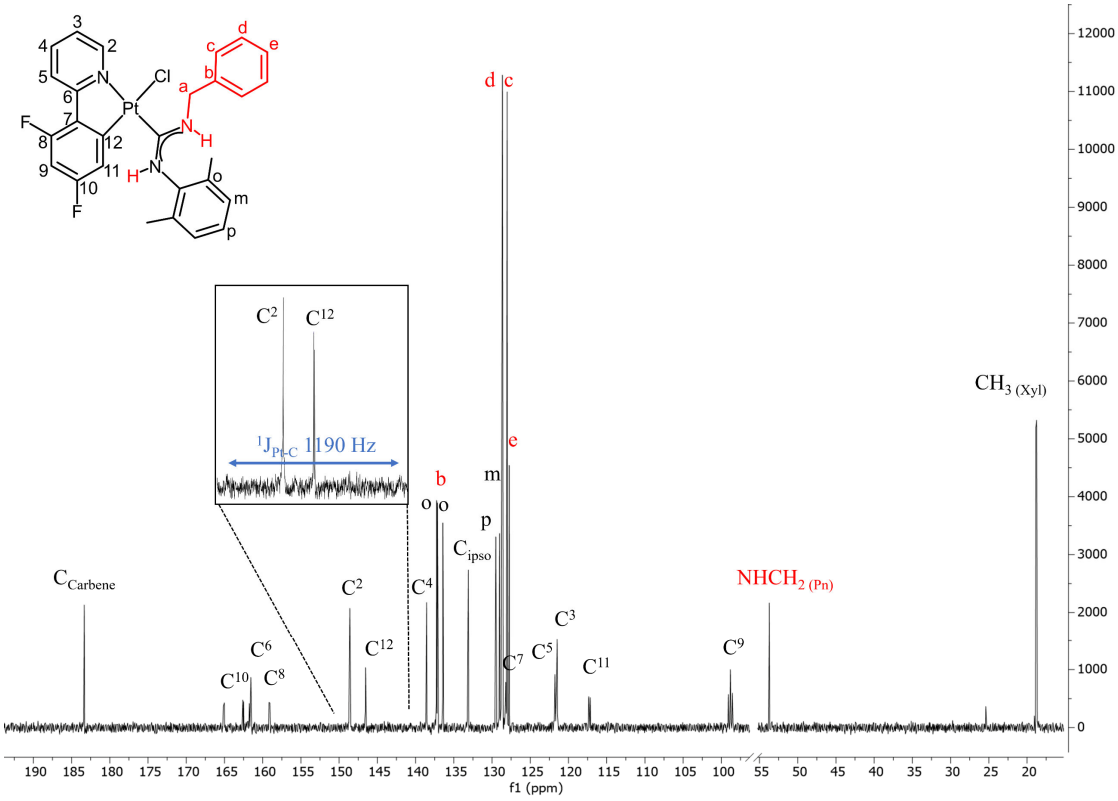

(b)

Figure S3. a) Selected region of the ^{1}H NMR spectra of [Pt(dfppy)Cl{C(NHXyl)(NHCH$_2$Ph)}] (**3b**) in $CDCl_3$ at 298 K with increasing complex concentration (*For a better visualization, the intensity of the 2.4 ppm section in relation to the rest of the spectrum is not real). b) ^{13}C{^{1}H} NMR spectra of **3b** in $CDCl_3$ at 298 K.

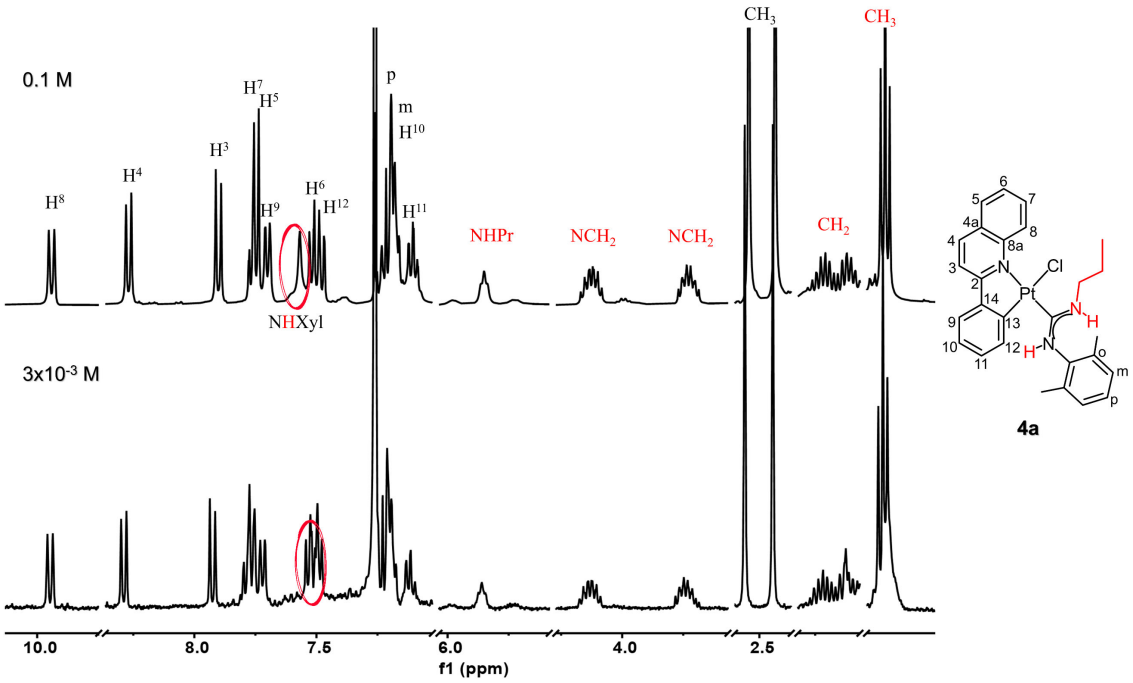

(a)

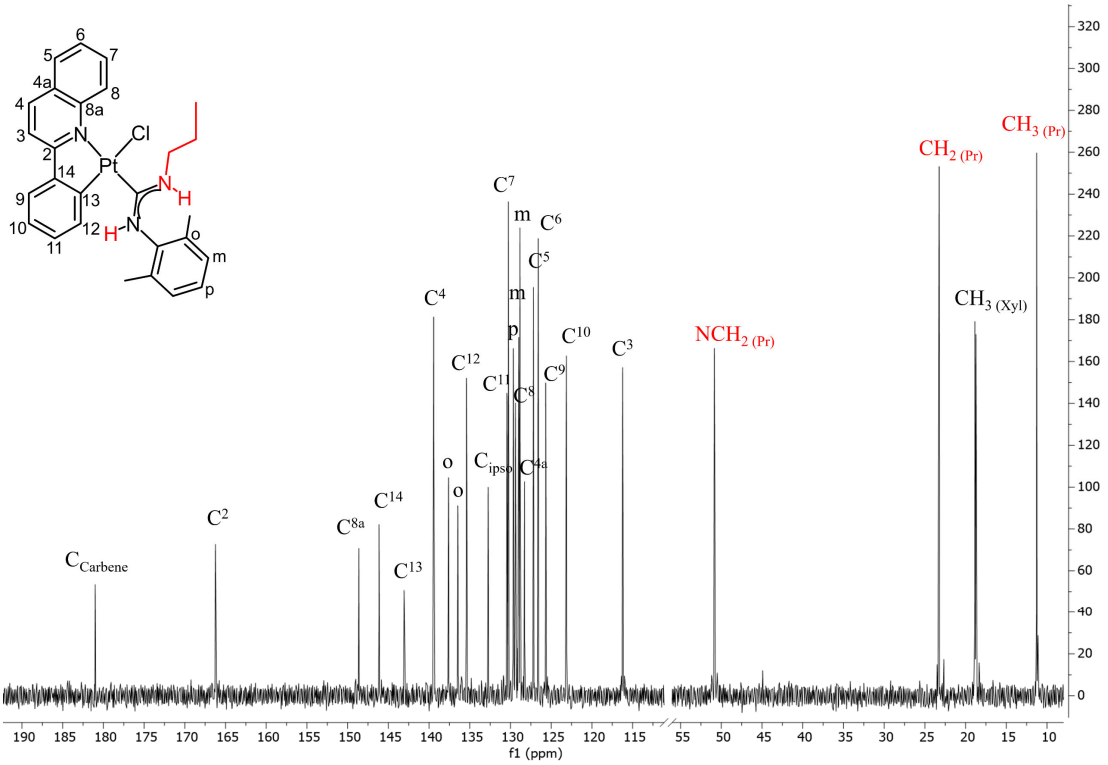

(b)

Figure S4. NMR spectra of **4a** in $CDCl_3$ at 298 K, (a) ^1H at two different concentrations, (b) $^{13}C\{^1H\}$.

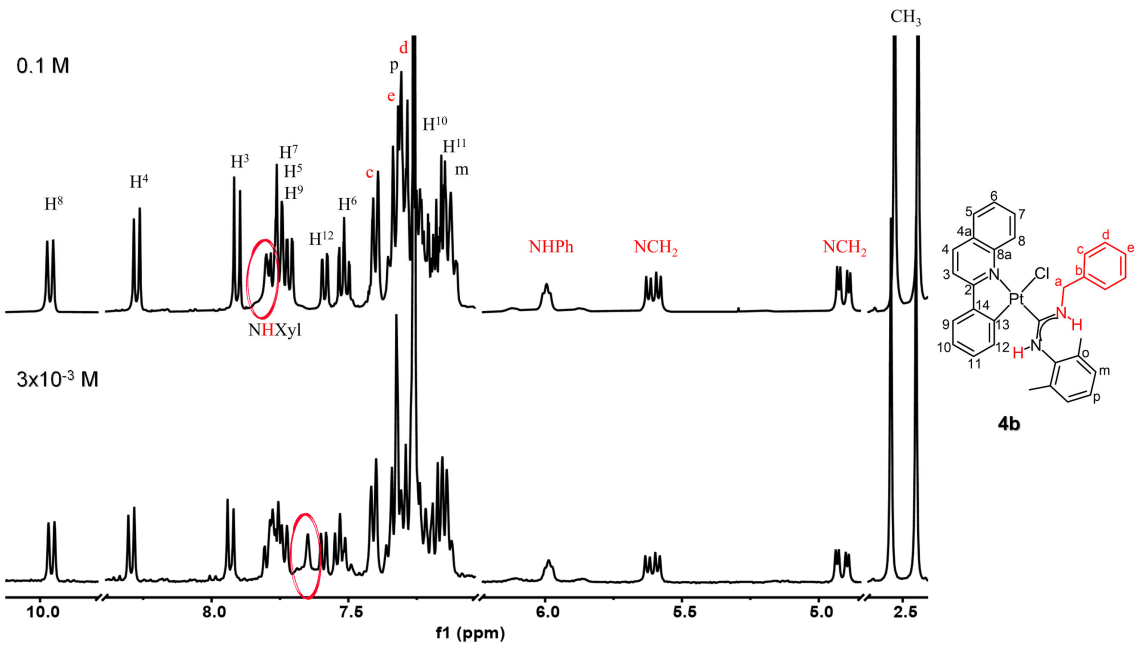

(a)

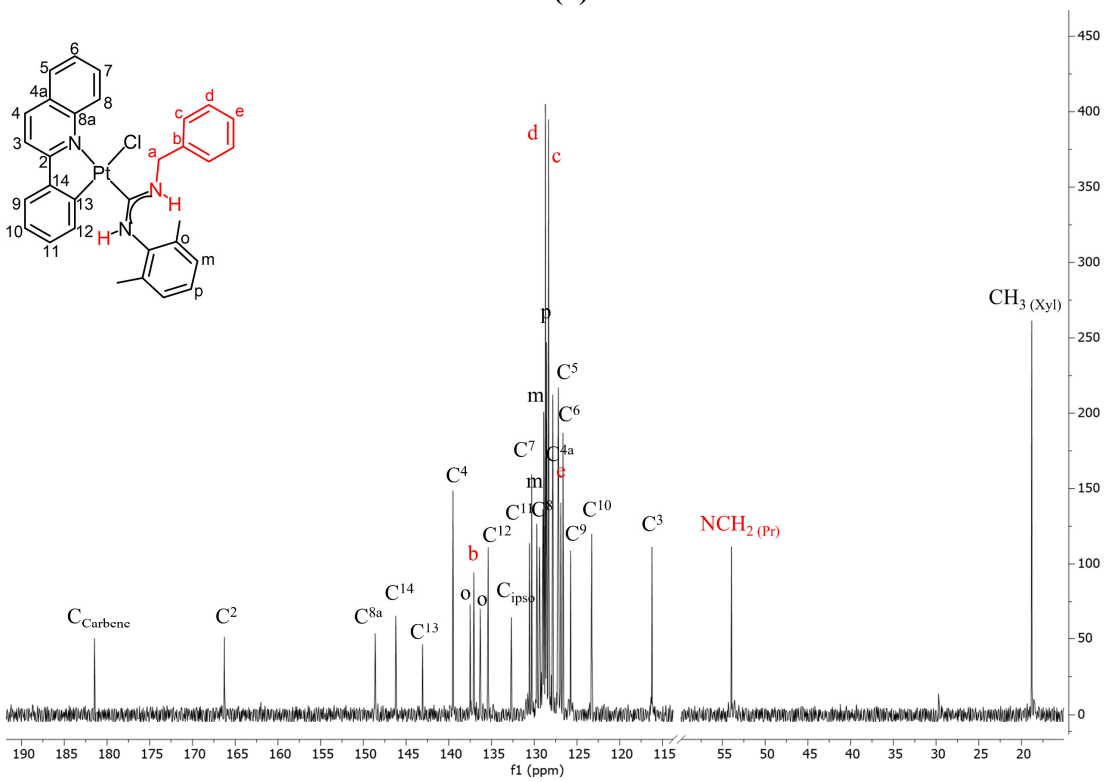

(b)

Figure S5. NMR spectra of **4b** in $CDCl_3$ at 298 K, (a) ^1H at two different concentrations, (b) $^{13}C\{^1H\}$.

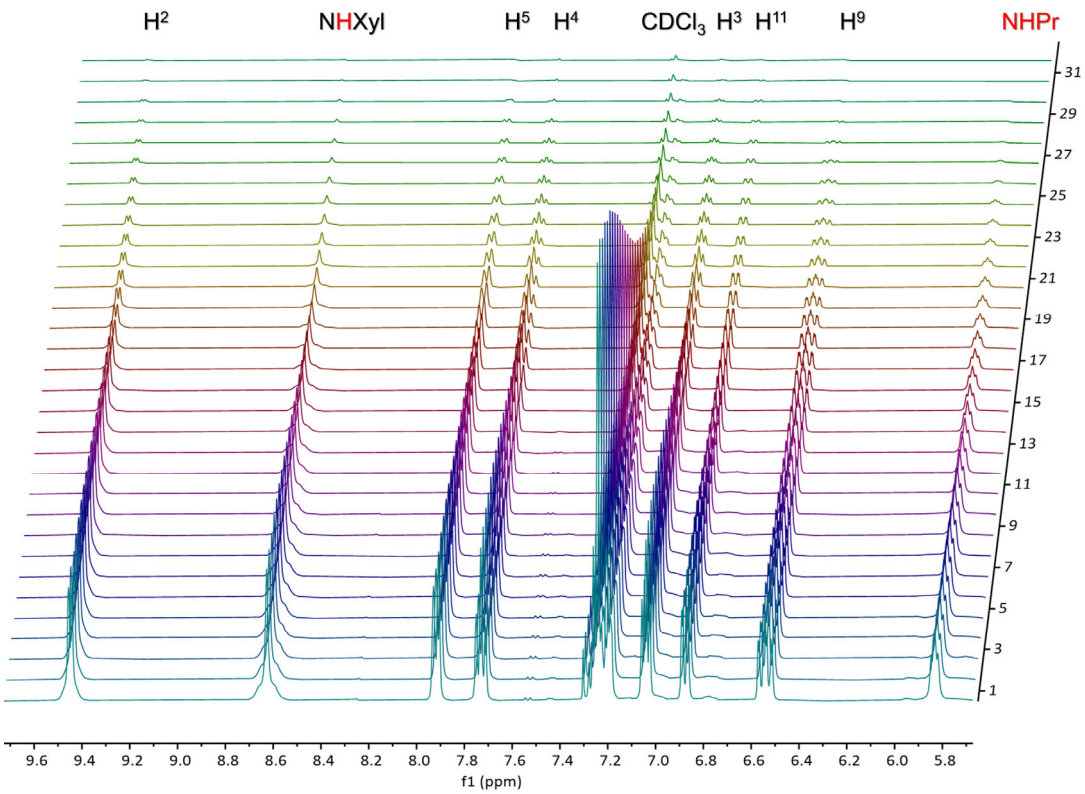

(a)

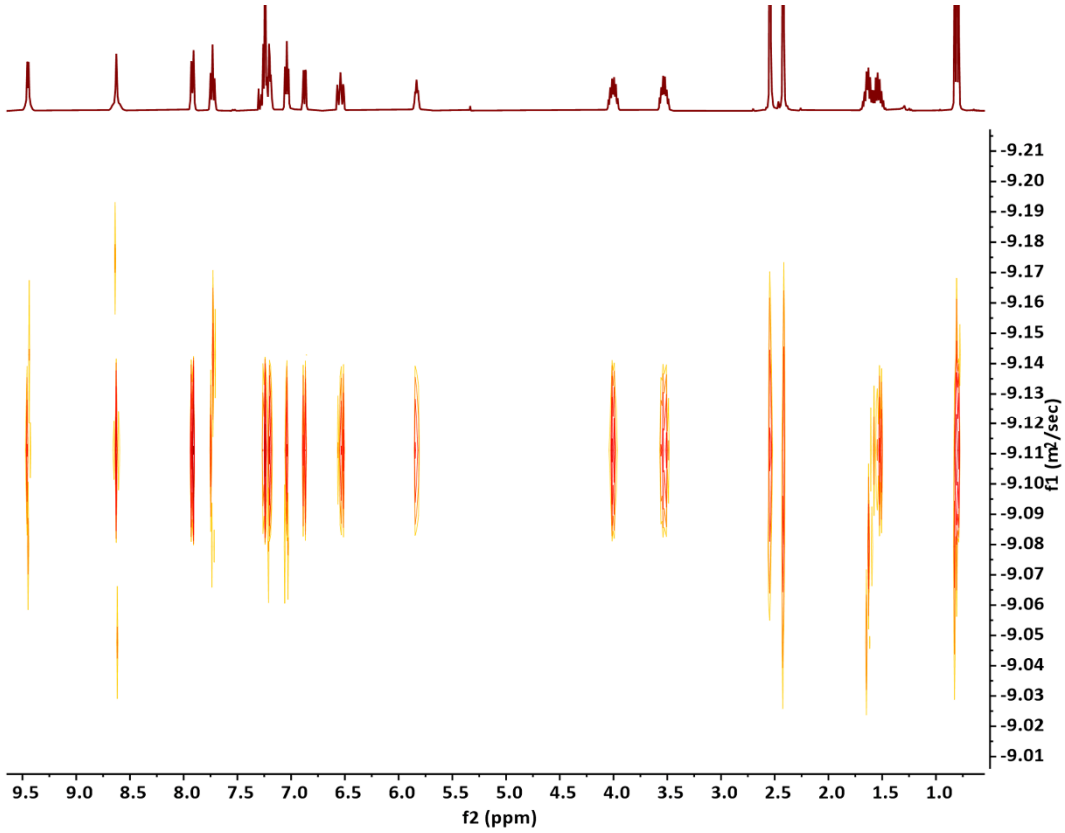

(b)

Figure S6. (a) Section of ^{1}H PGSE-NMR spectra for **3a** in $CDCl_3$ 0.1 M at 298 K. The resonance intensity of the H^2 signal decrease upon increasing the pulsed-field gradient (*g*). **(b)** ^{1}H DOSY NMR spectrum for **3a** in $CDCl_3$ 0.1 M.

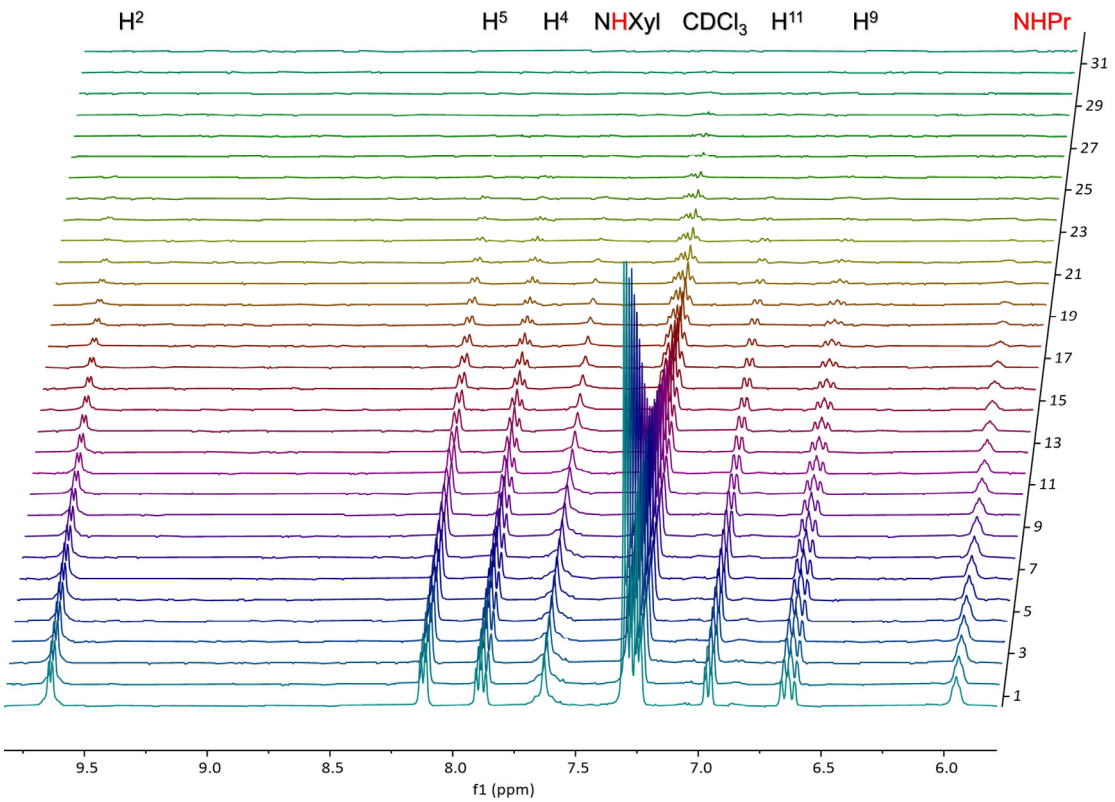

(a)

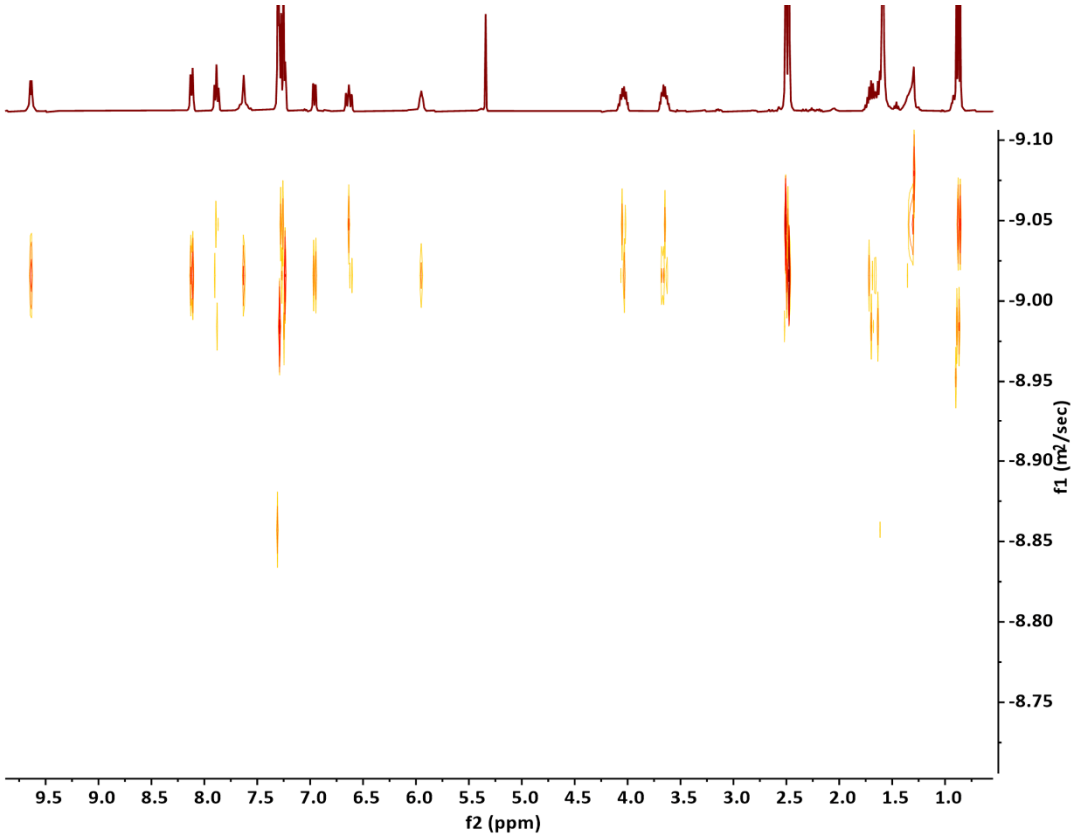

(b)

Figure S7. (a) Section of ^{1}H PGSE-NMR spectra for **3a** in $CDCl_3$ 3 x 10^{-3} M at 298 K. The resonance intensity of the H^2 signal decrease upon increasing the pulsed-field gradient (*g*). **(b)** ^{1}H DOSY NMR spectrum for **3a** in $CDCl_3$ 3 x 10^{-3} M.

1.3 Crystal Structures

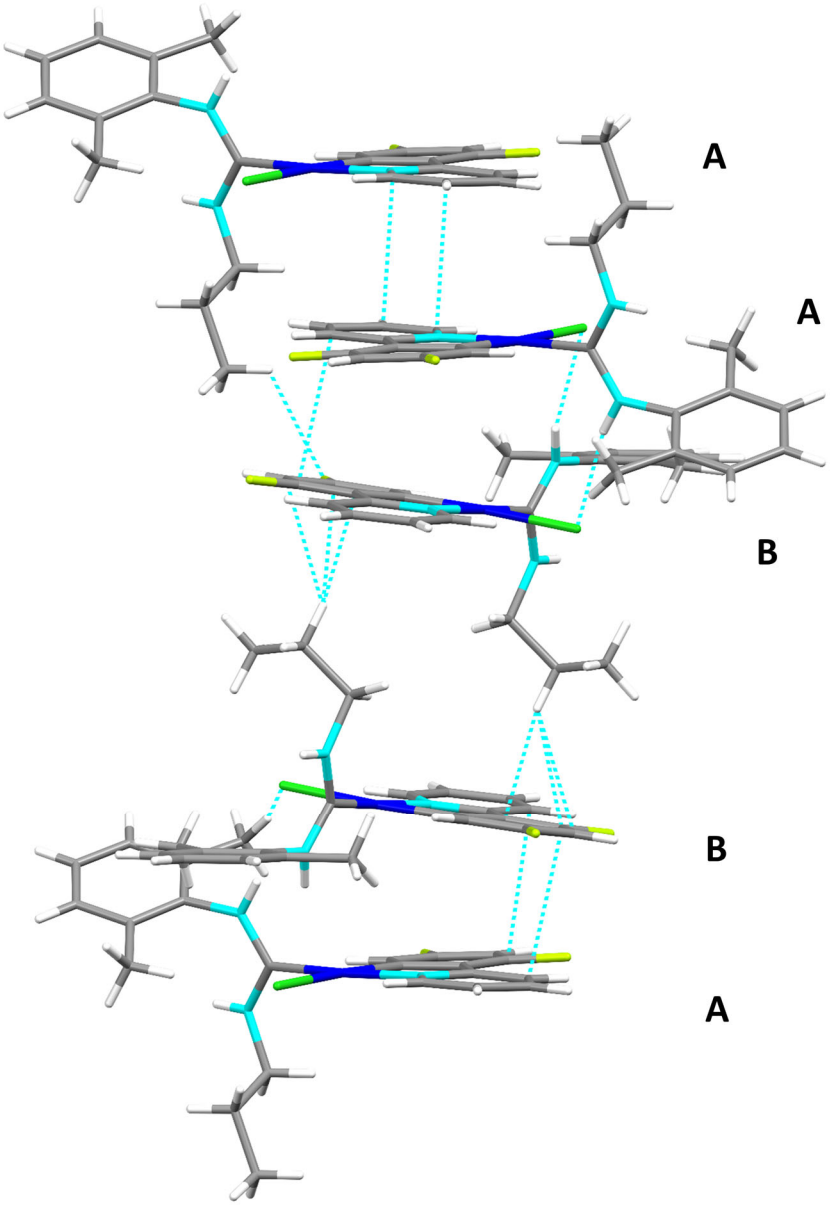

Figure S8. Crystal packing of complex **3a** showing head-to-head pairs of molecules (**A** and **B**) stacking in a columnar way with a sequence **AABBAA**…, viewed along the *c*-axis. The organization of **AA** molecules is supported by weak π···π interactions (3.407 Å), between **AB** molecules there are π···π interactions (3.45 – 3.42 Å) and secondary weak $NH_{(Xyl)}$···Cl (2.47, 2.36 Å), $NH_{(Pr)}$···F (2.77 Å) and $CH_{3(Xyl)}$···Cl (3.00 – 2.96 Å) contacts and between **BB** molecules there are $NH_{(Pr)}$···$\pi_{(dfppy)}$ interactions (2.98– 2.91 Å).

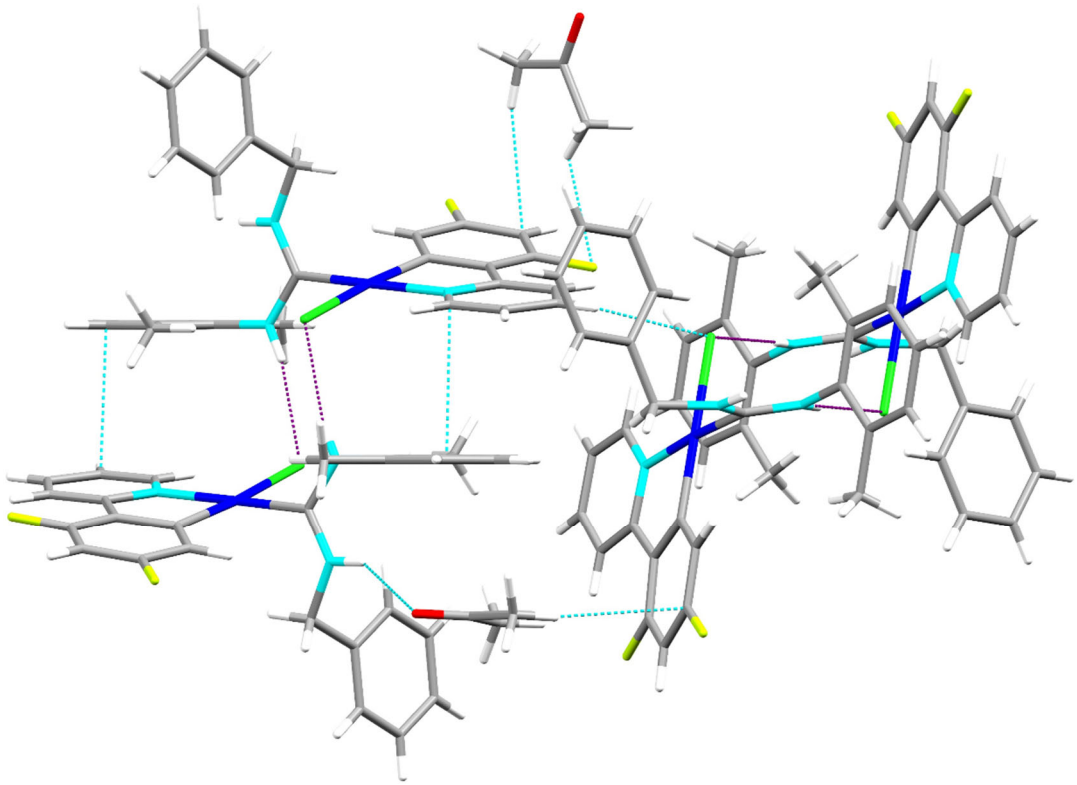

Figure S9. Crystal packing of **3b**·C_3H_6O showing head-to-tail pairs of molecules supported by intermolecular π···π interactions (3.42-3.33 Å) and by secondary weak $NH_{(Xyl)}$···Cl (2.427 Å) (purples lines) contacts, that connect with other dimers through weak Cl···$H_{(dfppy)}$ (2.921 Å). The crystal packing shows additional H(C_3H_6O)···F (2.567 Å), H(C_3H_6O)···$C_{(dfppy)}$ (2.77-2.41 Å) and O(C_3H_6O)···$NH_{(Benzyl)}$ (2.206 Å) intermolecular contacts.

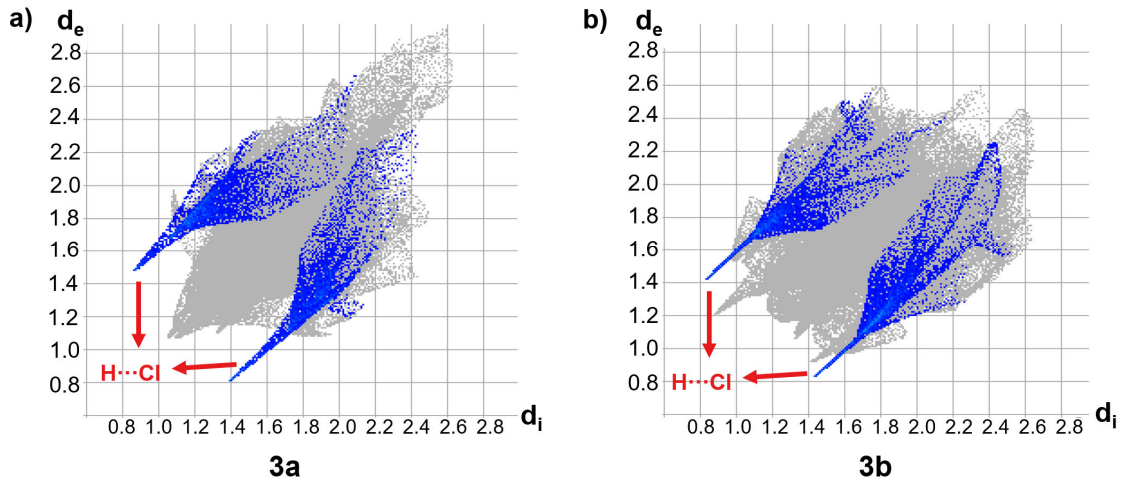

Figure S10. 2D fingerprint plots resolved into the H···Cl contacts: d_{norm} = normalized interaction distance, d_e= distance from the surface to the nearest nucleus external to the surface, d_i = distance from the surface to the nearest nucleus internal to the surface.

Table S1. X-ray Crystallographic Data for **3a** and **3b**·C_3H_6O.

	3a	**3b**·C_3H_6O
Empirical formula	C_{23} H_{24} Cl F_2 N_3 Pt	C_{30} H_{30} Cl F_2 N_3 O Pt
F_w	610.99	717.11
T (K)	145(2)	100(2)
Wavelength (Å)	0.71076	0.71076
Crystal system	Triclinic	Monoclinic
Space group	P -1	P 21/c
Crystal size (mm^3)	0.20 x 0.14 x 0.12	0.28 x 0.21 x 0.18
a (Å)	12.0987(16)	14.062(3)
b (Å)	12.5647(17)	10.476(2)
c (Å)	16.133(2)	19.364(4)
α (°)	103.864(4)	90
β (°)	97.365(4)	104.750(7)
γ (°)	108.330(4)	90
V ($Å^3$)	2204.4(5)	2758.7(10)
Z	4	4
D_{calcd} (Mg/m3)	1.841	1.727
Absorption coefficient (mm^{-1})	6.518	5.225
F(000)	1184	1408
θ range for data collection (deg)	2.877 to 26.732°	2.939 to 27.903°
Index ranges	-15<=h<=15, -15<=k<=15, -20<=l<=20	-18<=h<=18, -13<=k<=13, -25<=l<=25
Reflections collected	124249	138786
Independent reflections	9358 [R(int) = 0.0415]	6580 [R(int) = 0.0204]
Data / restraints/ parameters	9358 / 0 / 581	6580 / 0 / 351
Goodness-of-fit on F^2 [a]	1.077	1.063
Final R index	R_1 = 0.0156	R_1 = 0.0137
[I > 2σ(I)][a]	wR_2 = 0.0336	wR_2 = 0.0359
R indexes (all data)[a]	R_1 = 0.0193, wR_2 = 0.0345	R_1 = 0.0138, wR_2 = 0.0360
Largest diff. peak and hole (e. $Å^{-3}$)	0.785 and -1.063	0.653 and -0.931

[a] $R_1 = \sum(|F_o| - |F_c|)/\sum|F_o|$; $wR_2 = [\sum w(F_o^2 - F_c^2)^2/\sum wF_o^2]^{1/2}$; goodness of fit = $\{\sum[w(F_o^2 - F_c^2)^2]/(N_{obs} - N_{param})\}^{1/2}$; $w=[\sigma^2(F_o)+(g_1P)^2 + g_2P]^{-1}$; $P = [\max(F_o^2;0 + 2F_c^2)/3$.

Table S2. Selected distances (Å) and angles (°) for **3a** and **3b**·C_3H_6O

3a (molecule A)			
Distances (Å)		**Angles (°)**	
Cl(1)-Pt(1)	2.3939(6)	N(1)-Pt(1)-Cl(1)	94.48(6)
N(1)-Pt(1)	2.0786(19)	C(11)-Pt(1)-N(1)	81.03(9)
C(11)-Pt(1)	1.983(2)	C(12)-Pt(1)-C(11)	95.70(9)
C(12)-Pt(1)	1.983(2)	C(12)-Pt(1)-Cl(1)	88.86(6)
C(5)-C(6)	1.470(4)	N(3)-C(12)-N(2)	116.3(2)
C(12)-N(2)	1.338(3)		
C(12)-N(3)	1.333(3)		
3a (molecule B)			
Distances (Å)		**Angles (°)**	
Cl(2)-Pt(2)	2.3896(6)	N(4)-Pt(2)-Cl(2)	95.97(6)
N(4)-Pt(2)	2.072(2)	C(34)-Pt(2)-N(4)	80.72(9)
C(34)-Pt(2)	1.979(2)	C(35)-Pt(2)-C(34)	94.95(10)
C(35)-Pt(2)	1.977(2)	C(35)-Pt(2)-Cl(2)	88.30(7)
C(28)-C(29)	1.473(3)	N(6)-C(35)-N(5)	115.9(2)
C(35)-N(5)	1.337(3)		
C(35)-N(6)	1.332(3)		
3b·C_3H_6O			
Distances (Å)		**Angles (°)**	
Cl(1)-Pt(1)	2.3781(5)	N(1)-Pt(1)-Cl(1)	94.90(5)
N(1)-Pt(1)	2.0733(16)	C(11)-Pt(1)-N(1)	80.82(7)
C(11)-Pt(1)	1.9819(18)	C(12)-Pt(1)-C(11)	95.24(7)
C(12)-Pt(1)	1.9816(18)	C(12)-Pt(1)-Cl(1)	88.99(5)
C(5)-C(6)	1.471(3)	N(3)-C(12)-N(2)	116.72(16)
C(12)-N(2)	1.338(2)		
C(12)-N(3)	1.331(2)		

2.- Photophysical Properties and Theoretical Calculations

Table S3. Absorption data for compounds **3a**, **3b**, **4a** and **4b** (5×10^{-5} M Solutions)

Compound	Media	λ_{abs}/nm (ε x 10^{-3} M^{-1} cm^{-1})
3a	CH_2Cl_2	249 (41.8), 307 (9.4), 320 (10.8), 335 (5.1), 365_{sh} (3.8), 385 (3.3)
	THF	258 (59.1), 263_h (58.4), 308_{sh} (15.7), 320 (14.8), 342 (6.4), 398 (2.5)
	DMSO	262 (30.8), 267 (27.2), 272_h (23.5), 308_{sh} (9.0), 320 (8.5), 342 (4.8), 392 (2.9)
3b	CH_2Cl_2	248 (31.1), 307 (7.4), 320 (8.6), 335_{sh} (4.2), 366 (3.1), 385 (2.8)
	THF	252 (37.0), 306_{sh} (8.9), 320 (8.7), 341 (4.9), 397 (2.8)
	DMSO	262 (27.4), 267 (24.3), 272_h (20.4), 307_{sh} (8.3), 320 (8.2), 341 (4.6), 390 (2.7)
4a	CH_2Cl_2	263 (59.6), 284_{sh} (40.7), 305_{sh} (18.2), 335 (15.0), 350 (17.2), 431 (6.3)
	THF	260 (71.7), 287_{sh} (38.4), 311_{sh} (19.2), 335_{sh} (13.0), 351 (13.8), 444 (4.4)
	DMSO	265 (37.9), 286_{sh} (31.6), 313_{sh} (14.0), 336 (12.7), 351 (14.2), 437 (4.9)
4b	CH_2Cl_2	264 (42.7), 284_{sh} (33.4), 306_{sh} (15.8), 335 (11.7), 349 (13.1), 429 (4.5)
	THF	264 (55.8), 286_{sh} (39.4), 311 (18.1), 336 (13.3), 351 (14.7), 442 (4.6)
	DMSO	266 (48.4), 286_{sh} (35.1), 315_{sh} (15.6), 337 (12.8), 350 (13.6), 437 (4.3)

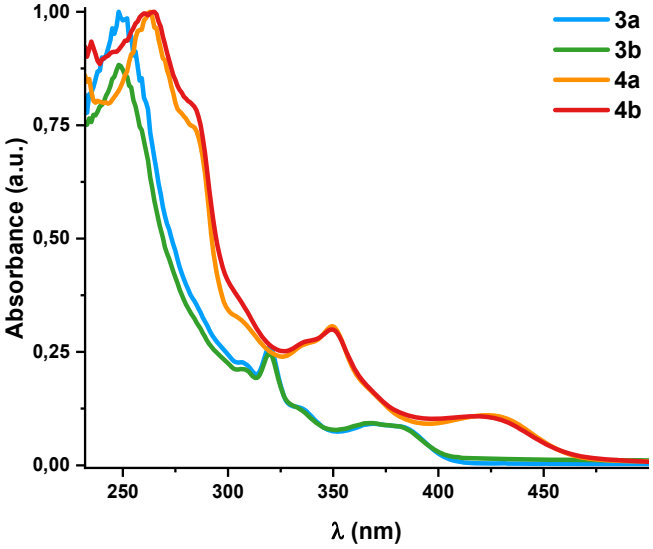

a)

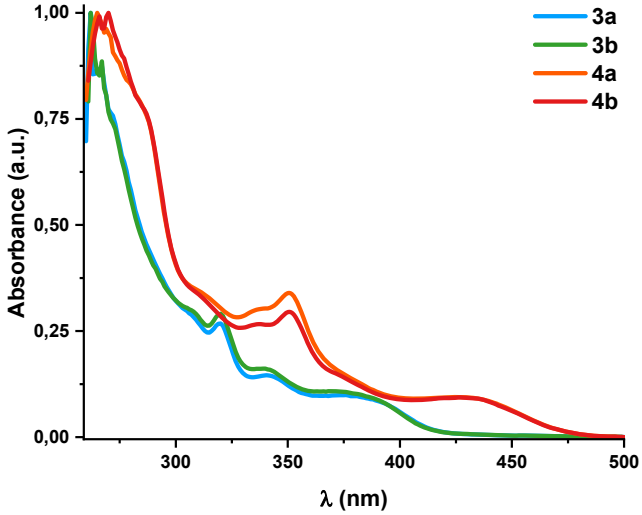

b)

Figure S11. Normalized absorption spectra of complexes **3a**, **3b**, **4a** and **4b** in a) CH_2Cl_2, b) DMSO (5×10^{-5} M).

Table S4. DFT optimized geometries for ground state and triplet state of **3a** and **4b** in THF.

3a

	X-ray (Molecule A)	S_0	T_1
Cl(1)-Pt(1)	2.3939(6)	2.503	2.498
N(1)-Pt(1)	2.0786(19)	2.124	2.093
C(11)-Pt(1)	1.983(2)	2.004	1.975
C(12)-Pt(1)	1.983(2)	2.006	2.020
C(5)-C(6)	1.470(4)	1.468	1.397
C(12)-N(2)	1.338(3)	1.353	1.351
C(12)-N(3)	1.333(3)	1.333	1.332
N(1)-Pt(1)-Cl(1)	94.48(6)	94.53	93.93
C(11)-Pt(1)-N(1)	81.03(9)	80.16	81.49
C(12)-Pt(1)-C(11)	95.70(9)	96.64	96.37
C(12)-Pt(1)-Cl(1)	88.86(6)	88.65	88.19
N(3)-C(12)-N(2)	116.3(2)	116.61	116.61

4b

	X-ray	S_0	T_1
Pt(63)-Cl(64)	-	2.562	2.541
Pt(63)-N(42)	-	2.209	2.101
Pt(63)-C(60)	-	1.998	1.986
Pt(63)-C(10)	-	1.996	2.019
C(5)-C(59)	-	1.467	1.420
C(10)- N(43)	-	1.354	1.352
C(10)- N(44)	-	1.332	1.331
Cl(64)-Pt(63)-N(42)	-	103.01	98.81
N(42)-Pt(63)-C(60)	-	79.42	80.92
C(60)-Pt(63)-C(10)	-	95.63	96.33
C(10)-Pt(63)-Cl(64)	-	81.93	84.21
N(43)-C(10)-N(44)	-	116.69	116.81

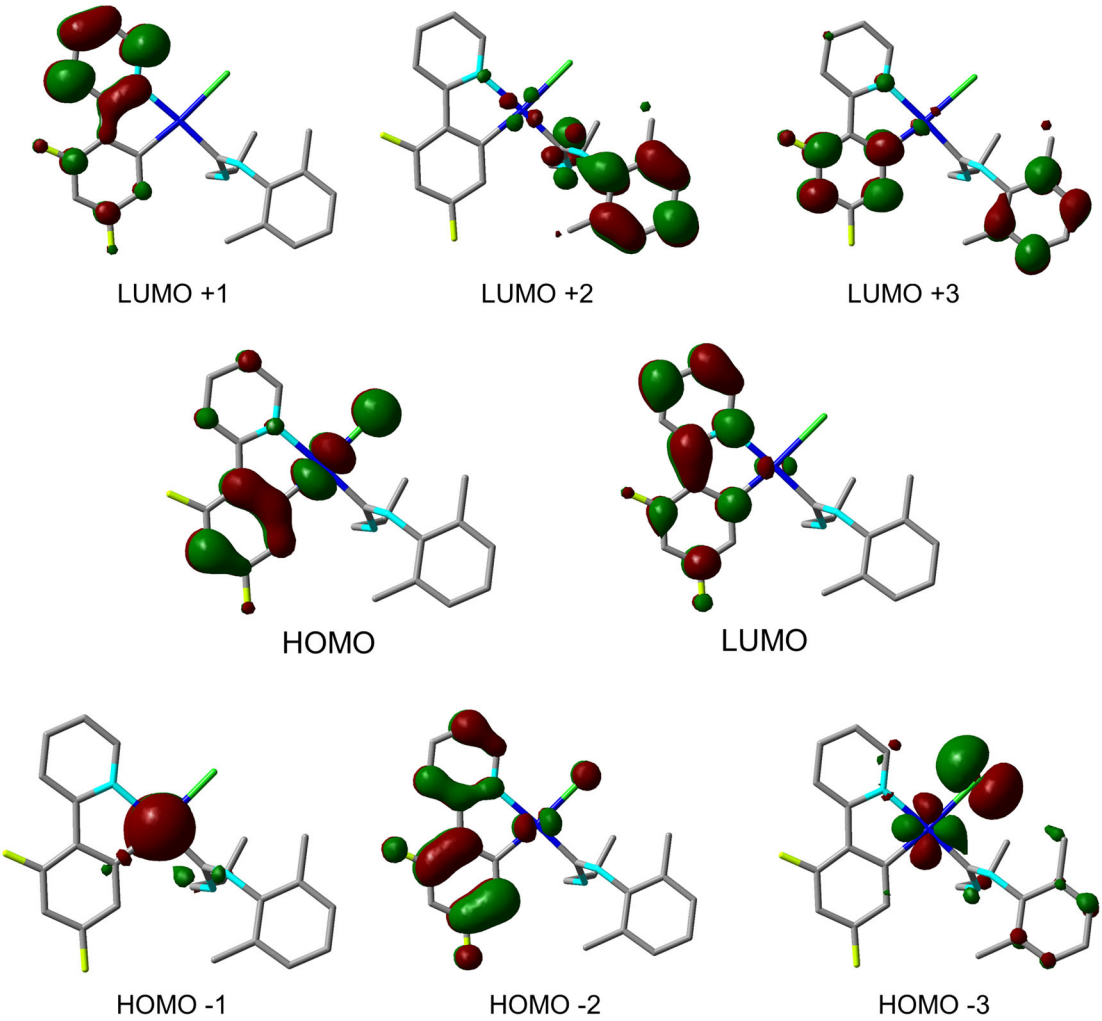

Figure S12. Selected frontier Molecular Orbitals for **3a** in the ground state.

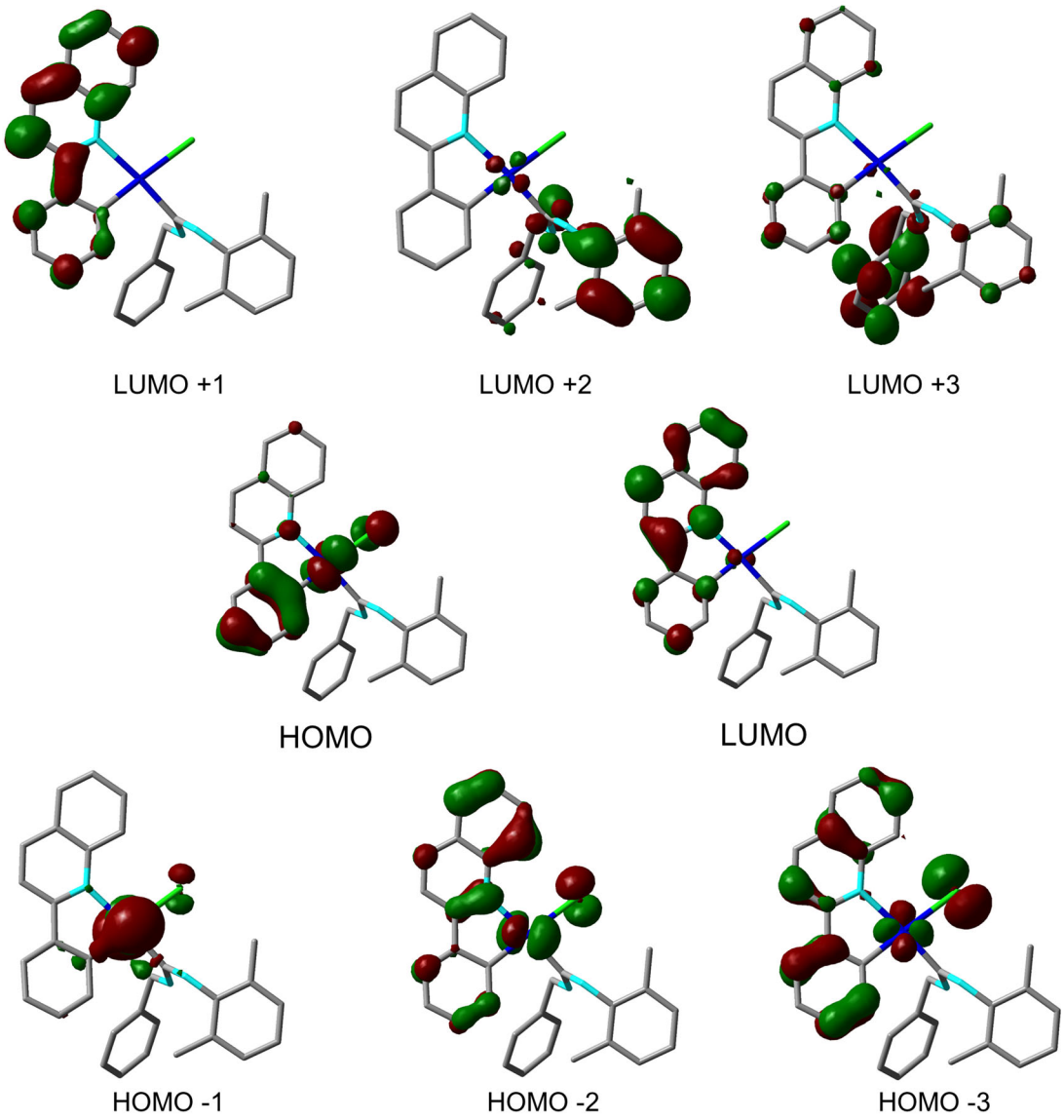

Figure S13. Selected frontier Molecular Orbitals for **4b** in the ground state.

Table S5. Composition (%) of Frontier MOs in terms of ligands and metals in the ground state for **3a** and **4b** in THF.

3a

MO	eV	Pt	dfppy	CNXyl	Propyl	Cl
LUMO+5	-0.12	36	24	30	5	6
LUMO+4	-0.20	6	28	65	1	0
LUMO+3	-0.22	9	50	40	1	0
LUMO+2	-0.54	5	4	87	3	1
LUMO+1	-0.92	1	99	0	0	0
LUMO	-1.68	6	92	1	0	0
HOMO	-5.83	40	45	0	0	15
HOMO-1	-6.20	90	4	3	2	0
HOMO-2	-6.39	7	88	0	0	5
HOMO-3	-6.60	25	4	10	2	59
HOMO-4	-6.72	3	1	92	0	5
HOMO-5	-6.80	15	4	68	13	1

4b

MO	eV	Pt	pq	CNXyl	Benzyl	Cl
LUMO+5	-0.17	15	43	24	17	1
LUMO+4	-0.24	4	1	25	69	0
LUMO+3	-0.40	10	18	12	59	0
LUMO+2	-0.54	5	3	83	8	1
LUMO+1	-1.00	1	99	0	0	0
LUMO	-2.02	4	95	0	0	0
HOMO	-5.67	38	51	0	0	11
HOMO-1	-6.07	79	10	3	3	4
HOMO-2	-6.22	26	61	1	0	12
HOMO-3	-6.45	11	59	2	0	28
HOMO-4	-6.56	19	35	14	8	24
HOMO-5	-6.69	1	5	76	16	2

Table S6. Selected vertical excitation energies singlets (S_0) and the first triplet computed by TDDFT/SCRF (THF) with the orbitals involved for **3a** and **4b**.

3a

	State	λ/nm	f	Transition (% Contribution)
3a	T_1	435.49	-	H-2→LUMO (22%), HOMO→LUMO (65%)
	T_2	365.35	-	H-2->LUMO (50%), HOMO->LUMO (29%), H-2->L+1 (7%)
	T_3	354.46	-	H-1→LUMO (96%)
	S_1	365.52	0.050	HOMO→LUMO (97%)
	S_2	339.96	0.0082	H-1→LUMO (99%)
	S_3	302.13	0.0907	H-2→LUMO (73%), HOMO→L+1 (18%)
	S_4	298.00	0.0001	H-3→LUMO (91%)
	S_5	294.74	0.0223	H-6→LUMO (19%), H-2→LUMO (11%), HOMO→L+1 (62%)
	S_6	282.03	0.2082	H-6→LUMO (48%), H-5→LUMO (13%), HOMO→L+1 (16%)
	S_7	281.23	0.0118	HOMO→L+2 (30%), HOMO→L+5 (55%)
	S_8	274.70	0.0024	H-1→L+1 (93%)
	S_9	273.39	0.0216	H-1→L+1 (23%), H-1→L+5 (59%)
	S_{10}	266.24	0.0019	H-5→LUMO (36%), H-4→LUMO (60%)
	S_{11}	264.89	0.0016	H-5→LUMO (42%), H-4→LUMO (44%)
	S_{12}	260.61	0.0290	H-7→LUMO (74%)
	State	λ/nm	f	Transition (% Contribution)
4b	T_1	506.14	-	H-2→LUMO (28%), HOMO→LUMO (55%)
	T_2	442.36	-	H-2→LUMO (36%), HOMO→LUMO (34%)
	T_3	393.91	-	H-1→LUMO (83%)
	S_1	418.75	0.0662	HOMO→LUMO (98%)
	S_2	382.12	0.0046	H-1→LUMO (95%)
	S_3	343.55	0.0575	H-2→LUMO (83%), H-3→LUMO (8%)
	S_4	325.70	0.1121	H-3→LUMO (77%), H-2→LUMO (8%)
	S_5	321.05	0.0565	H-4→LUMO (76%), HOMO→L+1 (14%)
	S_6	303.70	0.2101	HOMO→L+1 (79%), H-4→LUMO (10%)
	S_7	296.81	0.0087	H-10→LUMO (17%), H-9→LUMO (21%), H-6→LUMO (29%), H-5→LUMO (18%)
	S_8	290.25	0.0022	H-9→LUMO (36%), H-5→LUMO (49%)
	S_9	288.14	0.0076	HOMO→L+2 (32%), HOMO→L+7 (41%)
	S_{10}	285.59	0.0012	H-6→LUMO (59%), H-5→LUMO (19%)
	S_{11}	283.54	0.0037	H-10→LUMO (33%), H-7→LUMO (15%), H-1→L+1 (32%)
	S_{12}	283.34	0.0064	H-10→LUMO (11%), H-7→LUMO (13%), H-1→L+1 (47%)

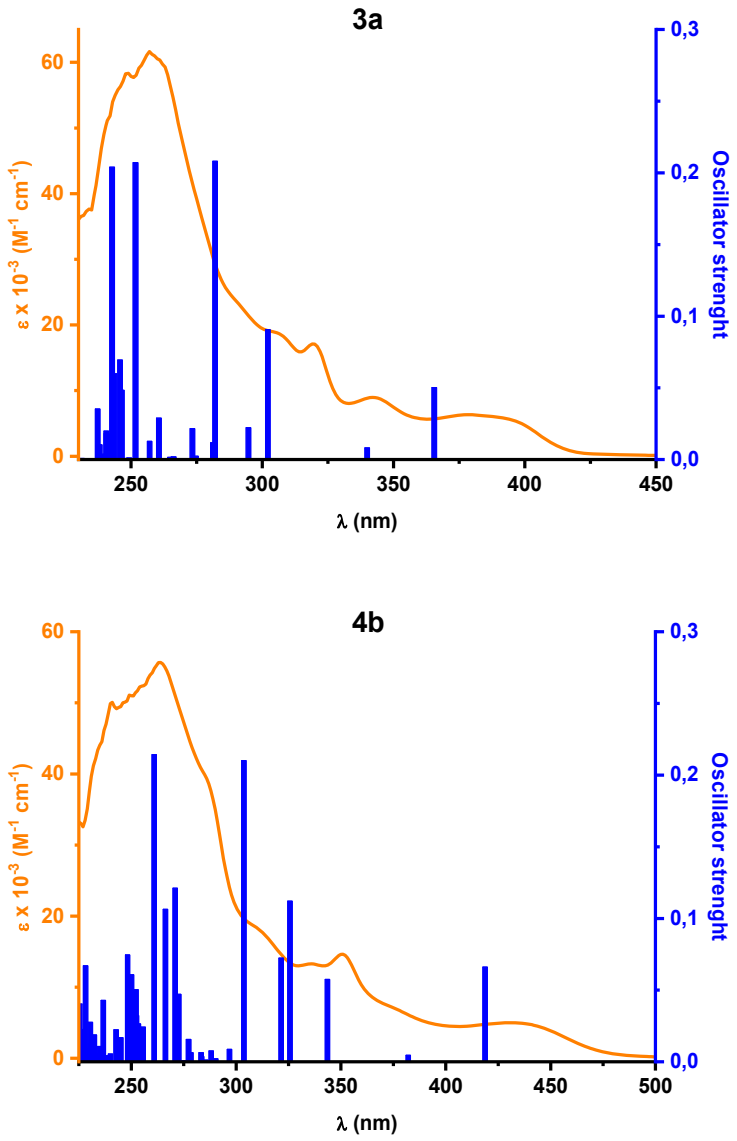

Figure S14. Calculated stick absorption spectra of **3a** and **4b** in THF compared with the experimental data.

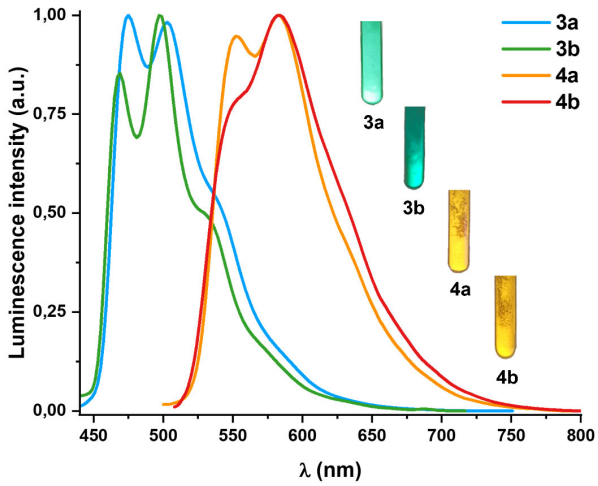

a)

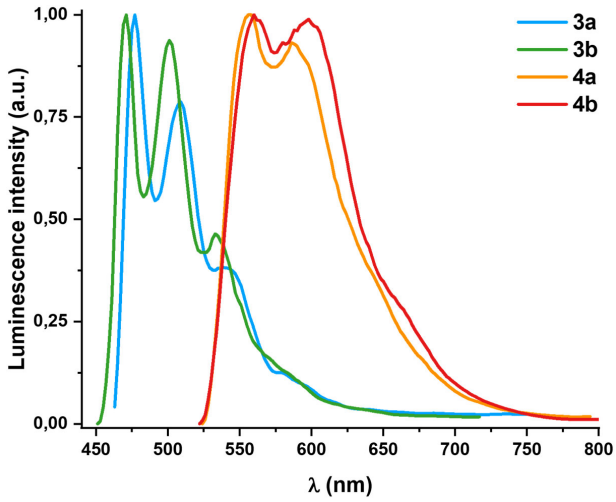

b)

Figure S15. Normalized emission spectra of all compounds in solid a) at 298 K, b) 77 K (λ_{ex} = 385 nm for **3a** and **3b**, λ_{ex} = 420 nm for **4a** and **4b**).

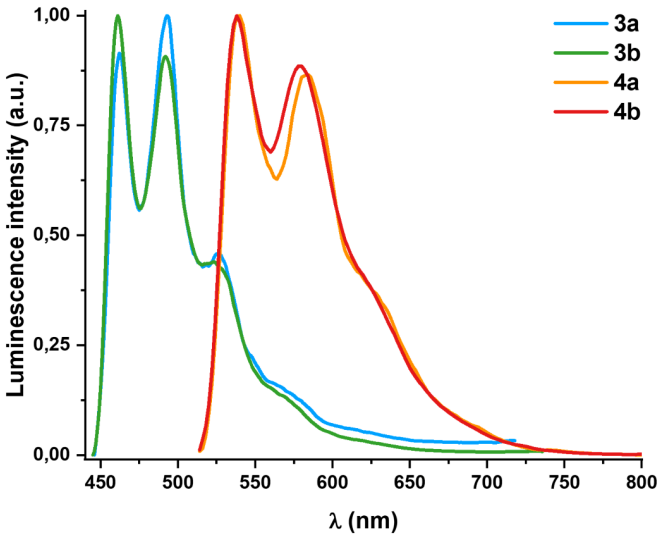

Figure S16. Normalized emission spectra of all complexes in THF at 77 K (λ_{ex} = 400 nm for **3a** and **3b**, λ_{ex} = 440 nm for **4a** and **4b**).

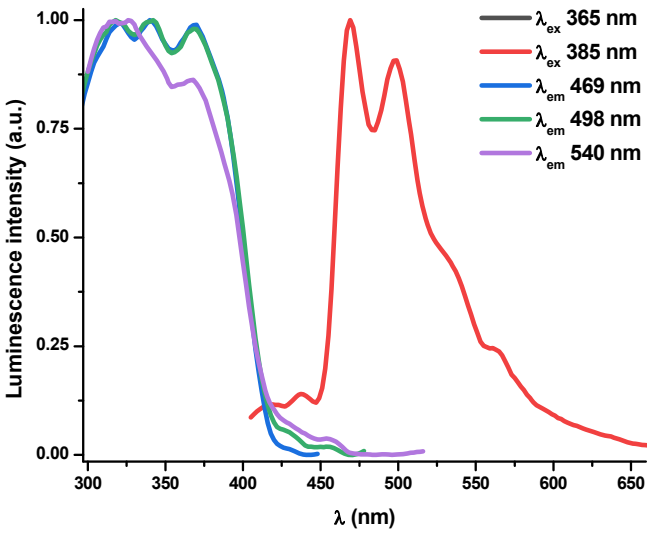

a)

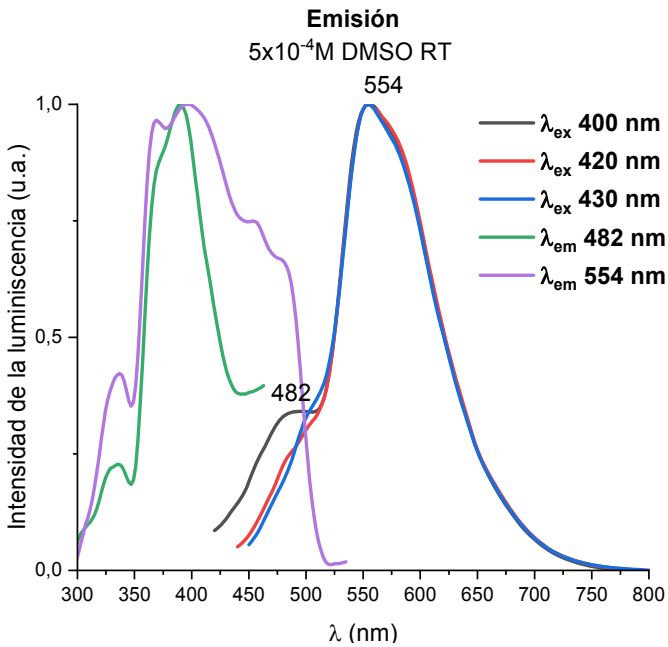

b)

Figure S17. Normalized emission spectra in DMSO (5 x 10^{-4} M) of a) **3a**, b) **4a**

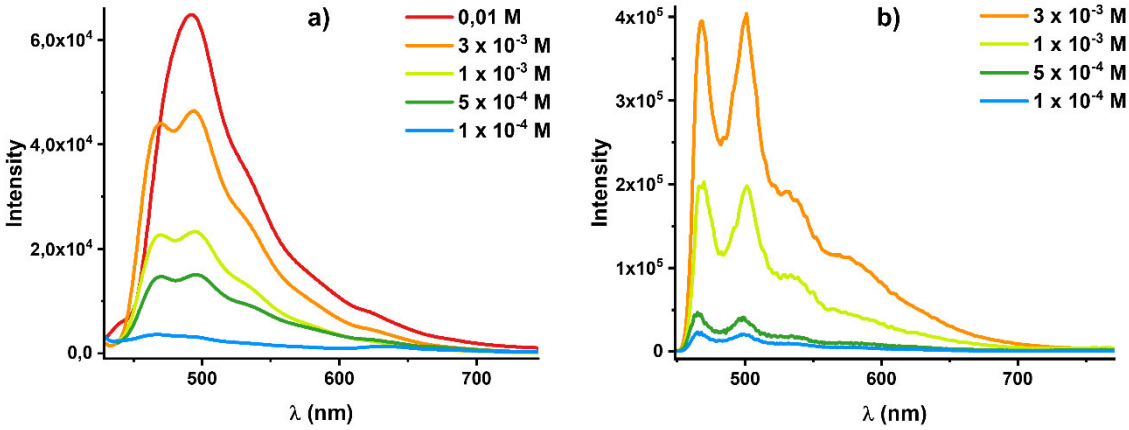

Figure S18. Emission spectra of **3a** in CH_2Cl_2 at different concentrations at a) 298 K and b) 77 K (λ_{ex} 400 nm).

Table S7. Composition (%) of Frontier MOs in terms of ligands and metals in the first triplet state for **3a** and **4b** in THF.

3a

MO	eV	Pt	dfppy	CNXyl	Propyl	Cl
SOMO	-3.33	6	93	0	0	1
SOMO-1	-4.40	14	84	0	0	2

4b

MO	eV	Pt	pq	CNXyl	Benzyl	Cl
SOMO	-3.68	4	95	0	0	1
SOMO-1	-4.34	14	84	0	0	1

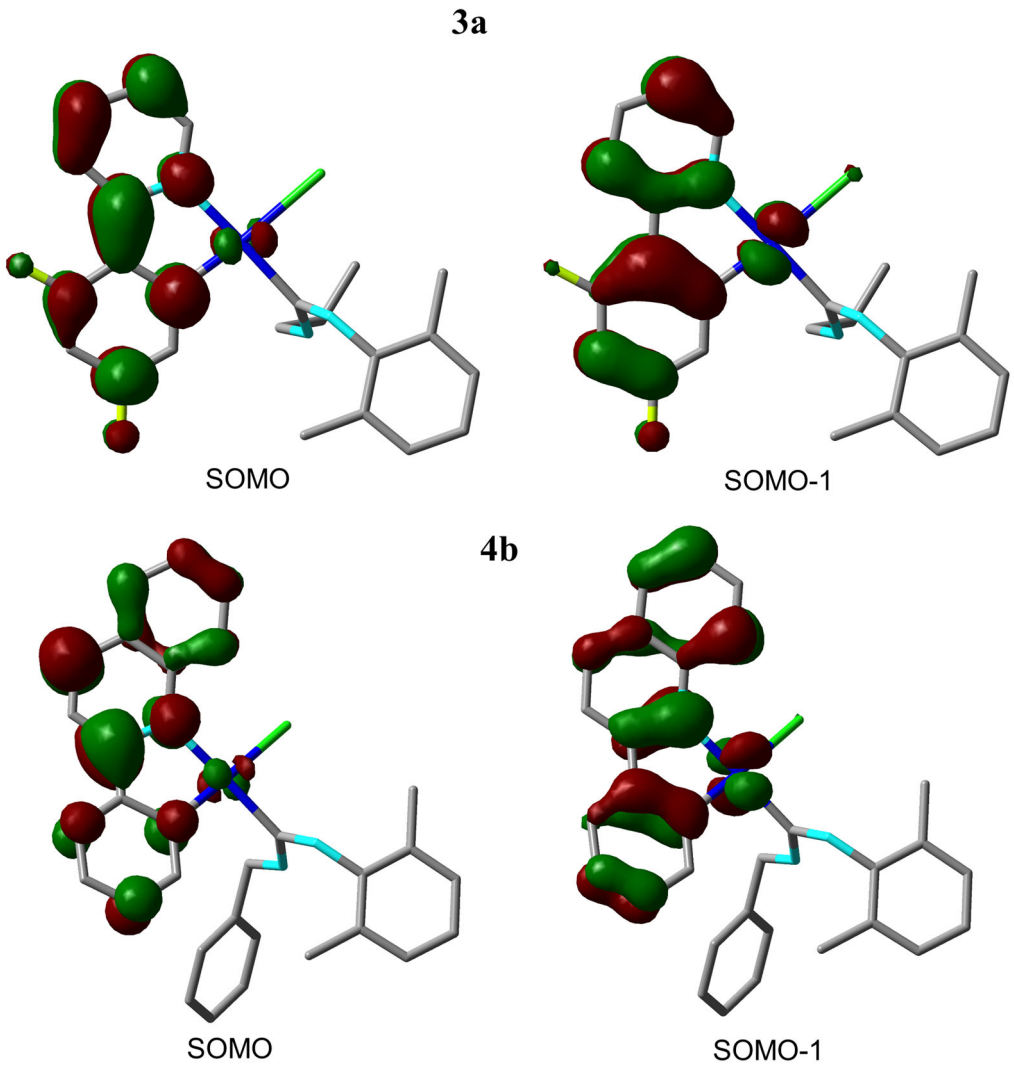

Figure S19. Frontier orbitals plots obtained by DFT for the first triplet state of **3a** and **4b**.

3.- Biological Studies

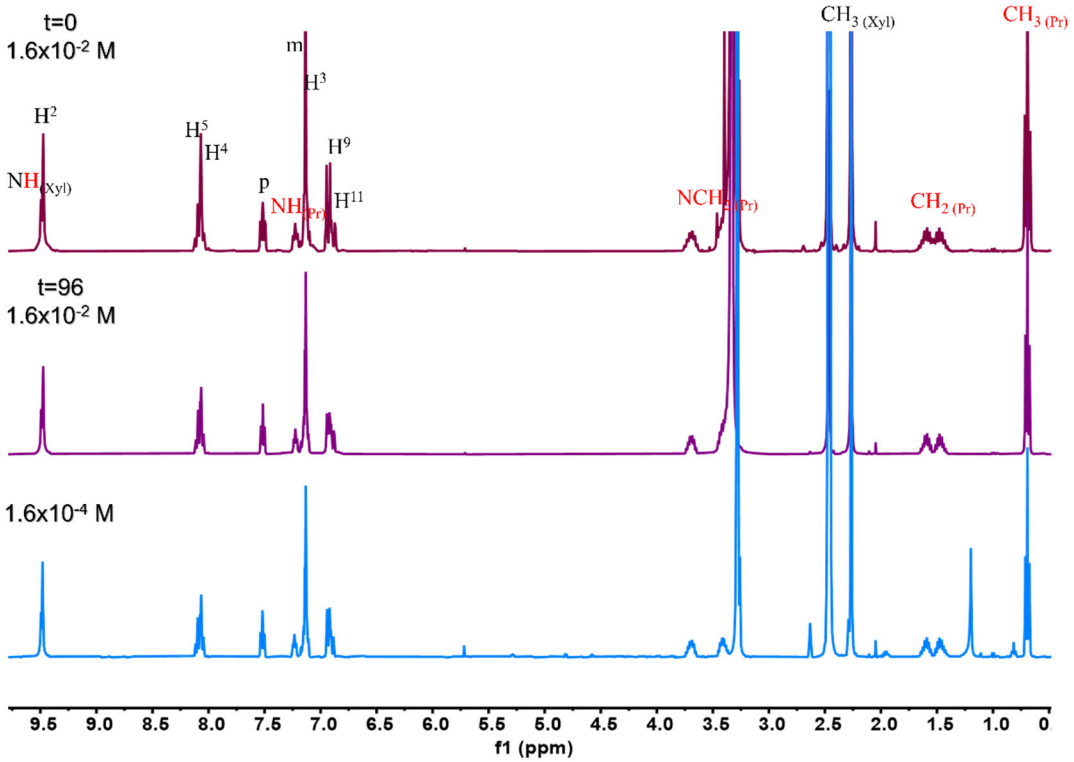

Figure S20. ^{1}H NMR spectra of **3a** in DMSO at 298 K at 1.6 x10^{-2} M (t = 0), (t = 96 h), and at 1.6 x 10^{-4} M

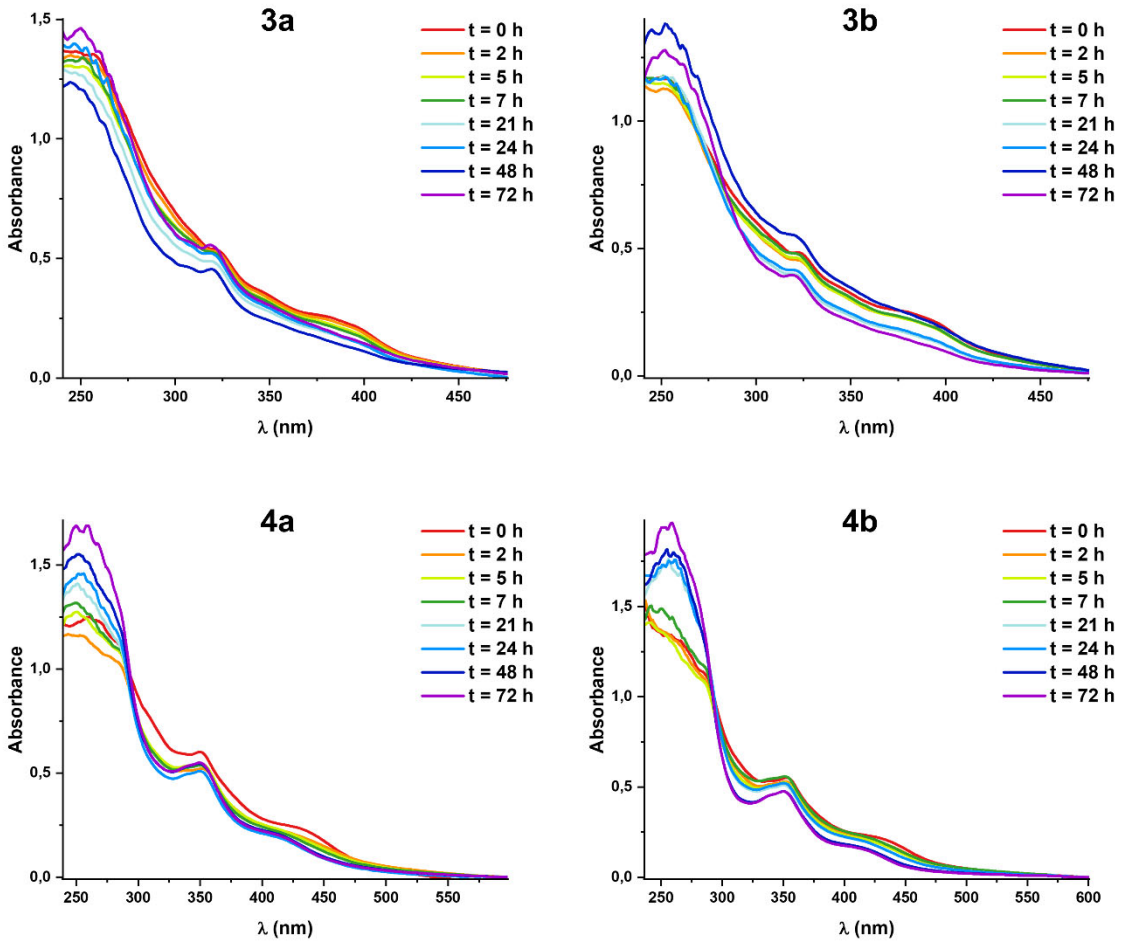

Figure S21. UV-vis absorption spectra of **3-4** (5 x 10^{-5} M) recorded in DMSO (<1%)-cellular medium after been kept at room temperature since 0 h to 72 h (intervals in legends).

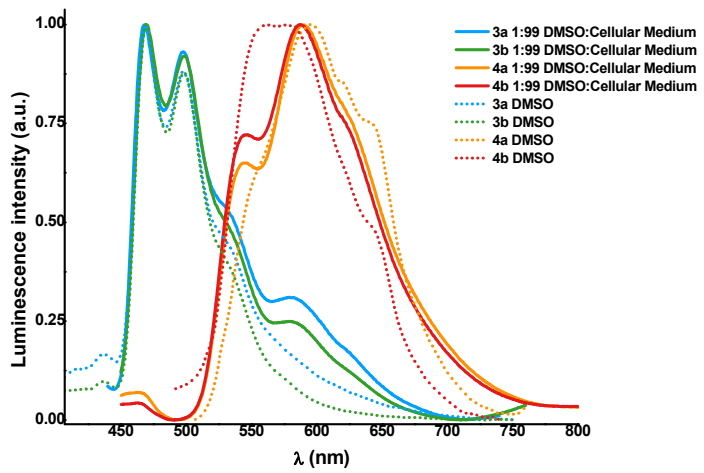

Figure S22. Emission spectra of all complexes in DMSO (dotted lines) and in 1:99 DMSO:celular medium used for MTT measurements (solid lines) (λ_{exc} 400 nm for **3** and 430 nm for **4**)

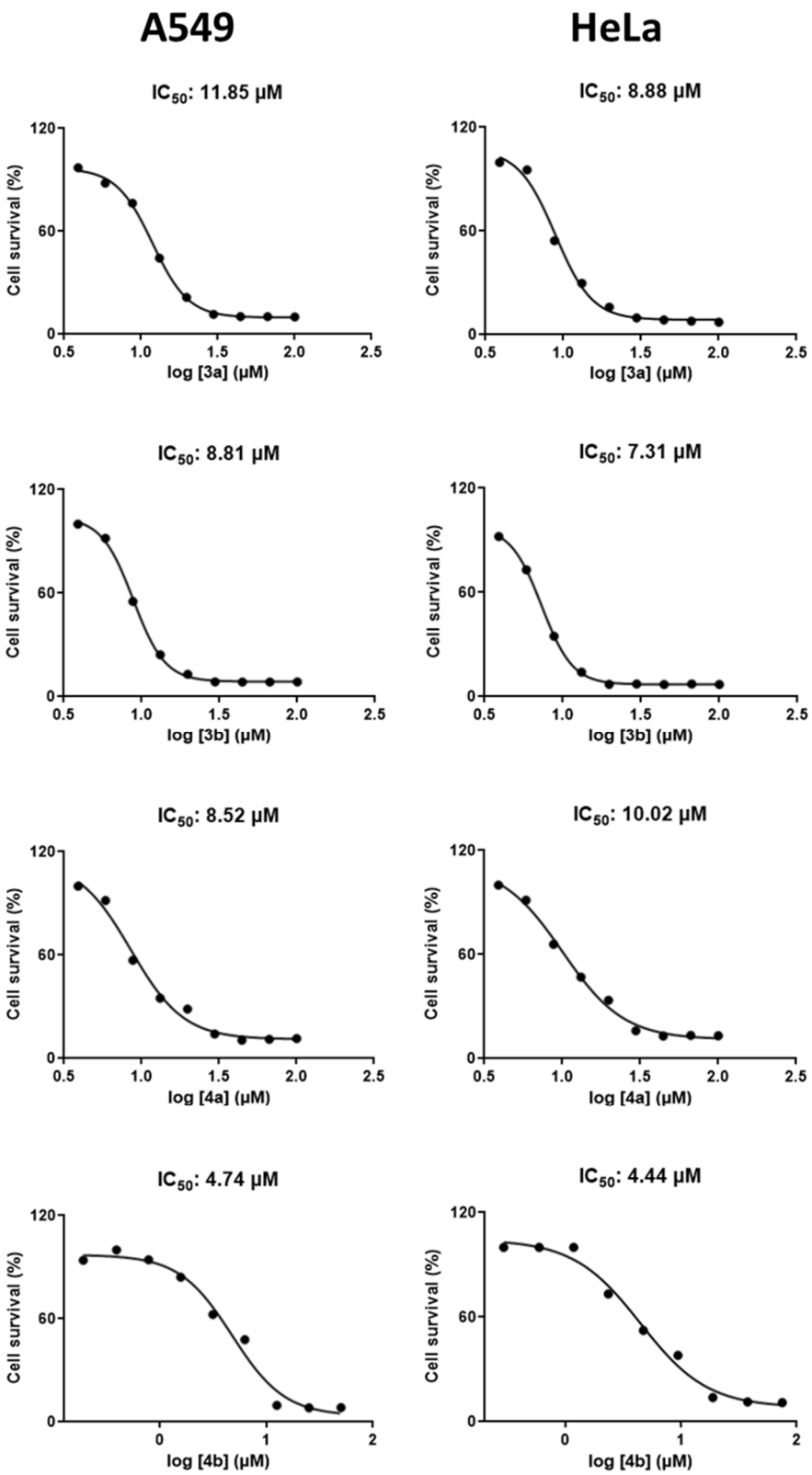

Figure S23. Dose-response curves for determination of the IC_{50} cytotoxicity values of **3a**,**b** and **4a**,**b** in A549 and HeLa cell lines. The IC_{50} values correspond to the dose required to inhibit 50% cellular growth, determined from the dose-dependence of surviving cells after cellular exposure to compounds for 72 h.